Experimental investigation of the flow evolution in the tributary of a 90° open channel confluence

S. Creëlle, L. Schindfessel, P. X. Ramos & T. De Mulder
Hydraulics Laboratory, Department of Civil Engineering, Ghent University, Ghent, Belgium

ABSTRACT: Open channel and river confluences have received a lot of attention in hydraulic literature, because of the interesting flow phenomena observed. Features such as flow acceleration, curvature, separation, mixing and recovery are combined in the confluence area into a complex 3D flow pattern. Typically, the analysis of these features is started at the upstream corner of the confluence area, and the upstream main and tributary branches are considered to be the (uniform) upstream boundary conditions. However, several indications in literature suggest the existence of flow features upstream of the confluence corner. This paper confirms, by means of measurements in a laboratory, 90° confluence flume, considerable streamline curvature in the tributary branch, upstream of the confluence. Furthermore, it shows and quantifies velocity redistribution as well as local water surface super-elevation and depression in the tributary branch. Consequently, flow feature analysis in confluences should start a considerable distance upstream of the confluence.

1 INTRODUCTION

Open channel and river confluences occur wherever two streams merge and continue downstream as one combined flow. This encounter imposes (strong) interaction of both incoming flows, caused by differences in flow direction, velocity, density, temperature etc. The combination of these gradients and the geometrical constraints results in a complex (3D) flow pattern that has triggered many researchers to study confluence hydro- and morphodynamics. Multiple influencing parameters have been uncovered, such as the confluence angle, incoming discharge (or momentum) ratio and presence of a bed discordance (e.g. Best 1985, Biron et al. 1996, Đorđević 2012). The main flow features identified are a mixing layer between the incoming flows, a separation zone starting at the downstream confluence corner and flow recovery downstream of the confluence (Best 1985). Classically, the existence of the mixing layer is explained by the difference in velocity between main and tributary channel inflow. As long as the difference in surface elevation between the incoming flows is limited, the velocity difference between the upstream branches is dominated by the discharge ratio (Weber et al. 2001).

However, several observations indicate that the flow just upstream of the confluence is disturbed and differs from the fully developed profile more upstream. Since in asymmetrical confluences mixing and shear layer characteristics can be significantly influenced by the lateral momentum flux (Rhoads and Sukhodolov 2008), the distribution of the incoming velocities over the tributary branch is key to understand downstream flow behavior.

The presence of the separation zone just downstream of the confluence causes the flow to accelerate towards the most contracted section. This acceleration is strongest at the wall of the tributary adjacent to the separation zone (right wall), and thus there the highest flow velocities are observed (Gurram & Karki 1997). A similar conclusion is found with the help of conformal mapping theory (Webber & Greated 1966). Since head losses in the tributary are small, the local acceleration along the wall is inseparable from local decreases in the water depth (Gurram & Karki 1997, Ramamurthy et al. 1988). At the opposing wall, a local decrease in flow velocities leads to locally increased water depths, giving rise to the formation of the stagnation zone. With conformal mapping theory, Modi et al. (1981) modeled the evolution of the location of this stagnation zone around the upstream corner, and conclude that the stagnation zone can intrude in the tributary for a significant distance in case of low tributary inflow.

Multiple authors established that together with the velocity redistribution process, a (local) deviation of the flow direction occurs, resulting in a discrepancy between the confluence angle and the inflow angle of the tributary to the main stream. The angle discrepancy has been found to be strongly de-

pendent on the discharge ratio (Đorđević 2012, Hager 1989, Hsu et al. 1998, Schindfessel et al. 2015).

The abovementioned observations are very similar to flow behavior observed upstream of river bend flumes. Although in that case the physical curvature of the flume is a discontinuous function, the streamline curvature is shown to have a more gradual transition. Because of this curvature, flow is redistributed over the flume, resulting in a free vortex profile at the beginning of the bend (Rozovskiĭ 1957), instead of the straight channel developed flow profile. Associated with this flow redistribution, a transversal water surface slope exists in a bend, similar to the water level differences observed in the tributary confluence channel.

2 OBJECTIVES

The present paper investigates the flow behavior in the tributary branch, upstream of the confluence in an experimental 90° confluence flume with fixed horizontal, concordant bed and rectangular cross-sections with equal widths. The main goal of this paper is to explore and quantify the streamline curvature, flow redistribution and local water surface depression and super-elevation in the tributary, known to exist from literature. Furthermore, it aims to assess the extent of the upstream influence of the confluence onto the tributary flow.

3 EXPERIMENTAL FACILITY

The data used in this study are gathered in a new confluence flume, located at the hydraulics laboratory of Ghent University. The flume is constructed entirely in polycarbonate, with an adaptable supporting structure, to offer the best visual access possible. The design was made to ensure good conditions for data acquisition with optical imaging techniques.
The flume is depicted in Figure 1. It has a fixed width of W=0.40 m, and the total length of the main channel is 12 m. The flow rates coming into the tributary (Q_t) and upstream main channel (Q_m) are measured by an electromagnetic flow meter . To obtain high quality instream conditions, in the upstream inlet facilities, the flow is guided through in total three grids, while being contracted towards the flume. The upstream main and tributary inlet sections are 3 m and 2.2m in length respectively, to allow the flow to develop before coming into the measurement domain. The downstream water level can be set with a controllable weir. A Cartesian coordinate system is introduced, with the origin in the middle of the tributary-confluence intersection. The x-axis is positive towards the downstream main channel, and the y-axis points upstream into the tributary.

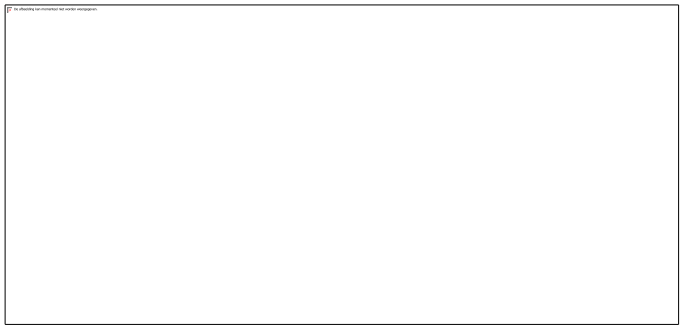

Figure 1. Schematized representation of the experimental flume. *(dimensions in m)*

4 MEASUREMENT METHODOLOGY

For the current objectives, three types of measurements will be performed. The first measurement is a (qualitative) visualization of the streamlines by the application of nylon wires to the flume. The wires are fixed on a small metal rod (3 mm diameter), mounted just downstream of the tributary inlet, near the bed. The wires show slightly negatively buoyant behavior in still water, thus staying near the bed during measurements. They are however still light enough so even very low flow is sufficient to change their position.

The second type of measurements is a velocity measurement, performed with a Valeport Electromagnetic Current Meter (ECM). The ECM has a measurement volume with a diameter of 2cm and a height of 1cm. In the current paper, velocity measurements were performed with the centre of the sampling volume at 60% of the water depth above the bed.

The third measurement device, applied to obtain the water depths, is an automated traverse system with an electronic measurement needle. The needle emits an electric pulse when making contact with the water. A linear actuator moves the electronic point gauge up and down, and logs the position of the needle the moment it pulses. To ensure small surface disturbances and high-frequency scale depth fluctuations do not influence the measurement accuracy, every depth measurement is recorded as the average of 20 repetitive measurements. For each measurement, the needle moves up again and waits briefly, to minimize the effect of surface tension.

The procedure gives a reproducible accuracy of 0.1 mm above a still water level, and measurements in the sampled flows are reproducible up to 0.2 mm. Absolute water levels are measured with a manual needle gauge, and prove reproducible up to 0.5 mm.

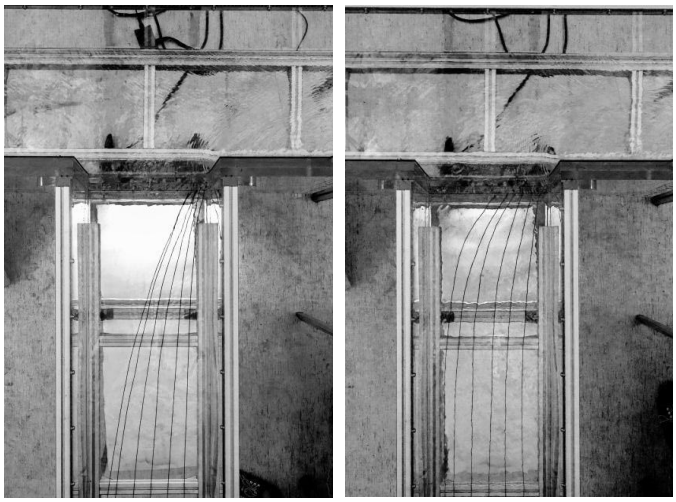

Figure 2. Visualization of the streamlines in the tributary for the relative flow rate q=0.25(left) and q=0.75 (right).

All the measurements are taken for a fixed total downstream flow rate $Q_d = Q_{t+} Q_m$=20 l/s . Two values of the relative flow rate q, defined as:

$$q = \frac{Q_t}{Q_d}, \quad (1)$$

are chosen to be 0.25 and 0.75. These cases represent a main channel dominant and a tributary dominant flow configuration respectively. For the current experiments the downstream weir was completely lowered, in order to minimize the water depths and maximize the quantities measured. This leads to upstream tributary water depths of 0.112 m and 0.113 m for q=0.25 and q=0.75 respectively. The obtained Froude numbers are 0.11 and 0.32, while the Reynolds numbers (defined as Re=4*A*U/ P ν are 32,000 and 96,000.

5 RESULTS

In this section, the measurement results will be presented for the two relative flow rates. To facilitate easy comparison of measurements between the relative flow rates, figures will be presented in pairs, with on the left a figure for q=0.25, while on the right results for q=0.75 are shown.

5.1 *Streamlines*

Figure 2 shows a top-down photographs of the nylon wires in the tributary, clearly visualizing the streamlines. Curvature of the streamlines can be clearly observed close to the confluence, and extends to a considerable (≈1 m for q=0.25 and ≈0.4 m for q=0.75) distance upstream in the tributary. Furthermore, a clear contraction of the wires towards the downstream corner can be observed, indicating the flow acceleration described in literature. The angle of the tributary streamlines to the main channel is clearly lower than the 90° physical confluence angle.

When comparing the results for both relative flow rates, the streamline contraction is far more pronounced for the case of q=0.25. This is in line with the results of Modi et al. (1981), stating that the stagnation zone moves into the tributary for low q. For the case of q=0.25, the contraction of the streamlines is so severe that at the confluence interface they only cover about 25% of the tributary width anymore. However, this observation can only be made near the bed, since this is where the wires are mounted. Possibly, at higher depths, the wires would behave differently.

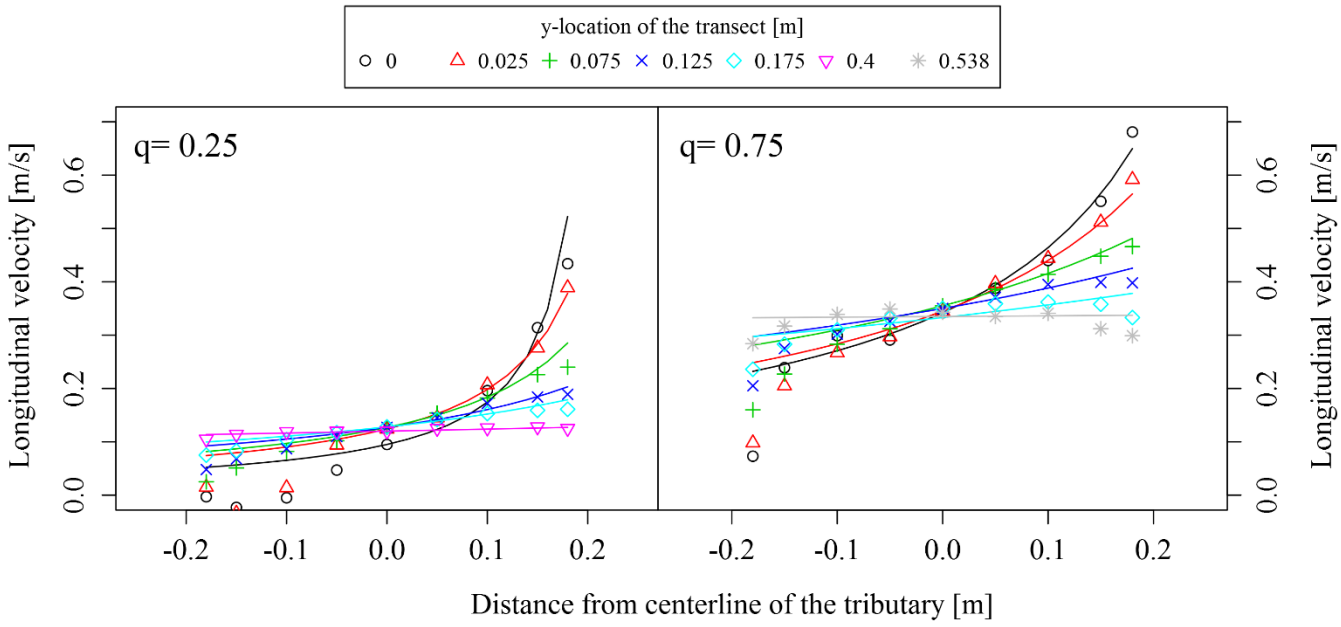

Figure 3. Measured(points) and modeled(lines) velocity profiles for a selection of tributary transects.

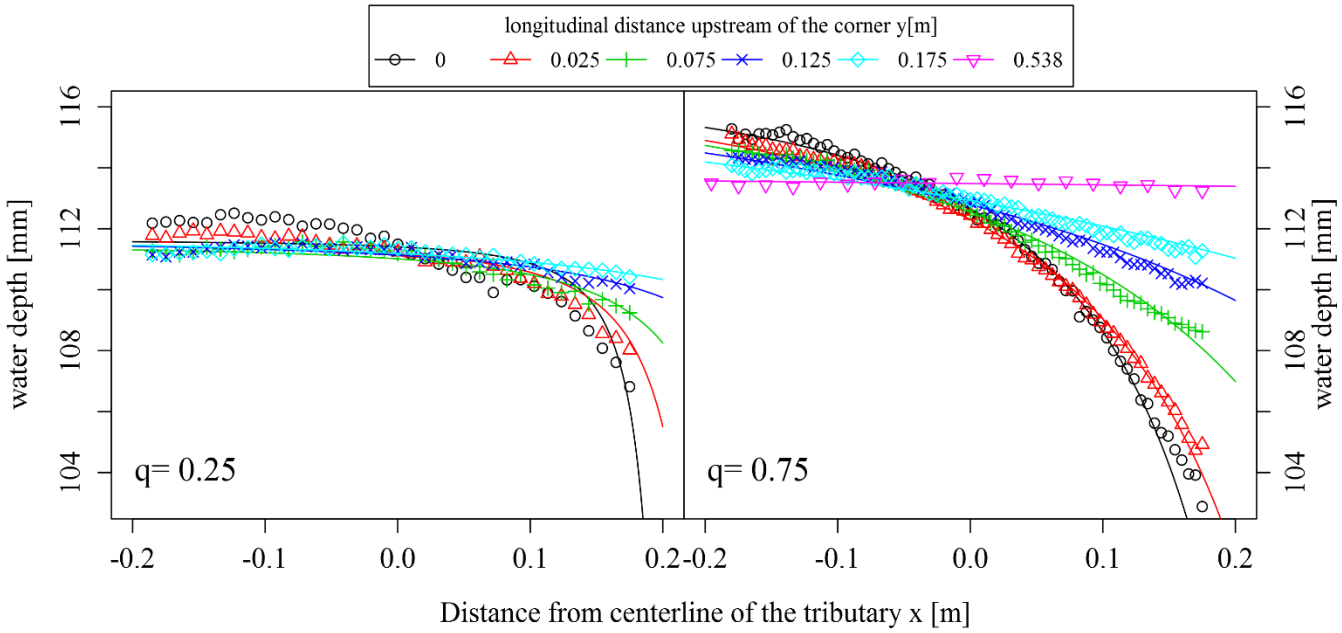

Figure 4. Measured (points) and modeled (lines) water heights for a selection of transects in the tributary.

$$v(x,y) = \frac{V(y)R(y)}{R(y)-x} \quad (2)$$

5.2 *Velocities*

Velocity measurements obtained with the ECM are presented by the points in figure 3. In the most upstream transects, the velocity profile is symmetrical over the width, with a clear uniform bulk velocity in the middle. Near the walls the velocity decreases somewhat, because of the boundary layer with the side walls. Profiles closer to the confluence (i.e. more downstream in the tributary) start to deviate from this profile, with higher flow velocities near the right wall, and lower velocities near the left wall. This is in agreement with the observations from the streamlines, that indicated a flow contraction towards the right wall (see Figure 2).

Comparing the results of the two relative flow rates, the expected difference in section-averaged flow velocity (imposed by the relative flow rate q) is apparent. However, while the velocities near the right wall in case of q=0.75 are clearly higher than for q=0.25, the relative acceleration for q=0.25 is significantly higher. On the left wall, for the case of q=0.75, the velocity gradually decreases, while for q=0.25 a more sudden, more pronounced decrease is present, with even negative velocities appearing. This means water from the main channel is flowing into the tributary, thus indicating in this case the stagnation point is certainly located within the tributary branch.

As indicated in the introduction, the pattern of redistribution in an upstream straight channel part is also observed in river bend flumes. In these bend flumes, the velocity profile near the transition from straight to curved channel can be described by the free vortex profile (Rozovskiĭ 1957):

with v the local velocity, R the radius of curvature at the transect centerline and V the transect-averaged velocity. Figure 3 presents the velocity profiles obtained with formula (2), with values of R fitted to obtain a good correspondence.

In general, the free vortex profile indeed seems to be a good approximation of the measured velocity profiles. Especially in the right part of the profile, where the contracting streamlines are present, the profile provides a very good match. On the left side, with the decelerating velocities, the formation of the stagnation zone seems to decelerate the velocities further than the profile predicts. Especially for q=0.25 the profile is a poor fit for the velocities encountered. Where the free vortex profile predicts velocities only slightly below the averaged velocity, measured velocities even go negative.

5.3 *Water depths*

Water depths, measured with the traverse-mounted gauge needle are presented in figure 4. A selection of measured water depths over a transect is depicted with points, clearly illustrating the evolution from the uniform water depth far upstream of the confluence, towards the specific profile at the confluence intersection. Approaching the confluence, a local surface depression develops near the right wall, becoming larger with decreasing distance towards the confluence. On the left wall, a surface elevation is distinguishable, albeit with a smaller amplitude than the surface depression on the right wall. This local super-elevation is indicative of the development of

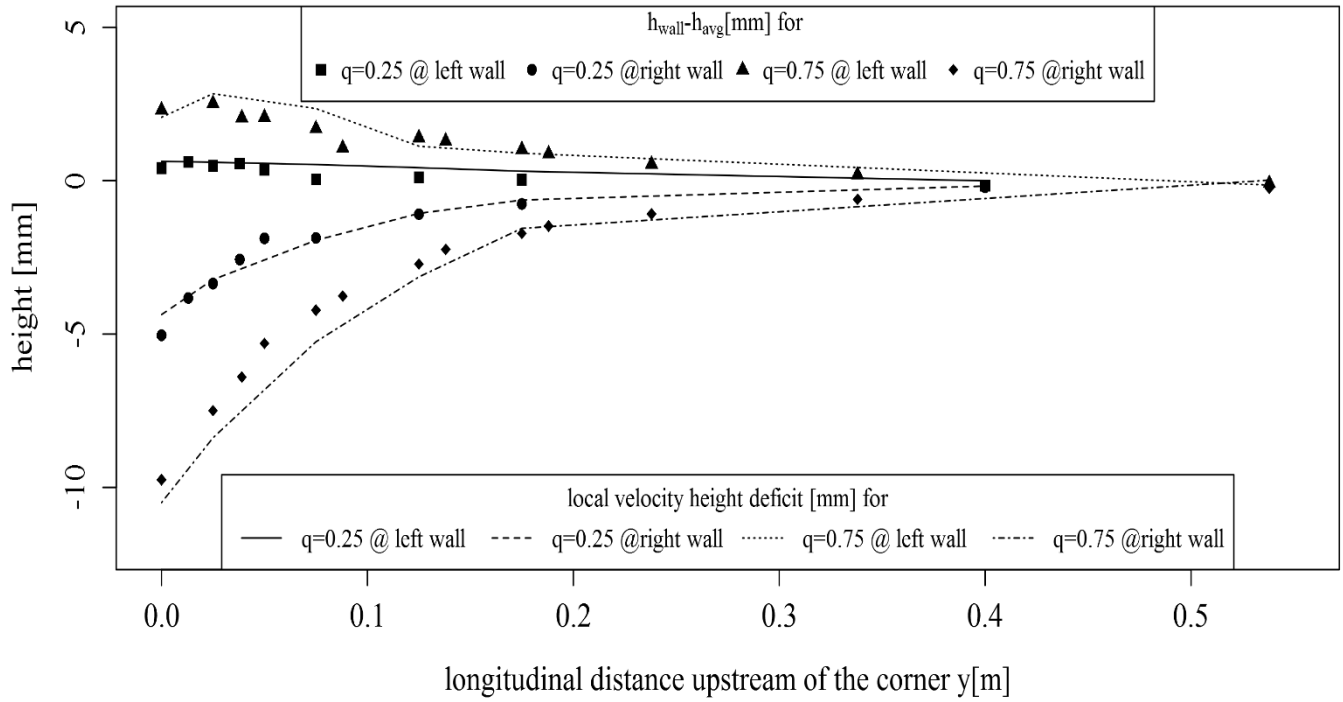

Figure 5. Comparison of local water depth difference(points) and the local velocity deficit (lines).

the flow stagnation zone near the left wall and the upstream confluence corner.

Comparing the measurements between the two flow ratios, two observations can be made. Although the total downstream flow is equal, average water depths in the q=0.75 are higher, as could be expected from literature on confluence head losses (Taylor 1944, Hsu et al. 1998). Secondly, water level differences between the left and right wall are far more pronounced for the higher relative flow rate.

5.4 *Energy height vs Water depth*

The flow in the tributary is adapting gradually, and velocity differences are limited. Assuming the energy head in a cross-section can be calculated with the section-averaged water depth and velocity, the local water depth can be expressed as the difference of the energy head and the local velocity head. With the free vortex profile approximation for the velocity profile introduced in paragraph 5.2, the predicted water depths are shown in full lines in figure 5. The overall agreement is good. Especially for the case of q=0.75, the predicted water depths have a very high agreement with the measurements. In case of q=0.25, some more discrepancies exist, especially in sections close to the confluence, where the local surface elevation near the left wall is somewhat underestimated (~1mm). This is in agreement with the results of the velocity predictions, where the local deceleration near the left bank was underestimated, and thus giving rise to un underestimation of the water depth predictions.

In order to evaluate the assumption that the local depression or super-elevation of the water level can be calculated as the difference of the energy head and the velocity height, figure 6 compares local water depth differences with local differences in the velocity height, calculated from the ECM measurements. It clearly shows that the velocity redistribution is indeed the dominant effect that causes the local depth differences, and energy losses in the tributary are quite limited.

6 DISCUSSION

The measurement results clearly show a significant effect of the confluence in the upstream tributary branch. In both cases of relative flow ratios, the nylon wires, visualizing the streamlines, show a clear curvature, that increases towards the confluence. This corresponds well to the findings with conformal mapping as reported in Webber & Greated (1965) and Modi et al. (1970).

However, while the wires give a qualitative understanding of the flow, they do not fully follow the flow because the location of the wire is not only influenced by the direction of the local streamline, but also by the drag forces more downstream, and the fact they are mounted near the bed.

The flow contraction towards the right wall is also clearly visible in the velocity transects. Velocities up to 1.8 times (for q=0.75) and 3.5 times (for q=0.25) the inlet tributary velocity are observed.

Measurements of the water depths clearly featured the elevated water depths near the tributary inner

wall, and the local surface depression near the tributary outer wall. The ratio of depth between the right and left wall at the confluence interface was investigated by Gurram & Karki (1997), and was defined as

$$\frac{h_{right}}{h_{left}} = 1 - 0.09\, q\, F_d \qquad (3)$$

with h_{left} and h_{right} the water depths at the left (upstream) and right (downstream) confluence corners.

For the current experiments, with $F_d \approx 0.5$ defined in an identical way as introduced in the original paper, this results in predicted depth ratios of 0.989 and 0.966 for q=0.25 and q=0.75 respectively. The measured depth ratios are however 0.947 and 0.896 respectively, where the latter is even lower than the lowest value of 0.91 that can be predicted with formula (3). Since the flume dimensions of both the experiments in Gurram & Karki (1997) and the current paper are comparable, differences cannot be attributed to different width-to-depth ratios or scale effects. Both flumes were constructed out of plastic material, and thus also differences in roughness should not cause differences of that order. A plausible explanation for the differences can however be sought in the difference in inlet sections and inlet conditions. Where in the current experiment the flow has about 2.25m (20h) between the last inlet guiding grid and the confluence area, the sketch of the facility used in Gurram & Karki (1997) suggests the inlet section is only 0.5 to 1m (5-10 times the water depth) away from the confluence section. Since the measured velocity profiles presented in this paper suggest the development of the free vortex profile is initiated a considerable distance upstream, the shorter development distance in Gurram & Karki (1997) might lead to a constrained development of the velocity profiles, forcing them more towards the uniform flow profile imposed at the upstream tributary inlet, and thus effectively reducing the velocity redistribution and associated differences in water depth.

The measurement data published by Weber et al. (2001) and simulated by Huang et al. (2002) allows for comparison of velocities as well as water depths. Both measurements and simulations indicate an upstream effect into the tributary, with the same patterns of flow contraction and water surface depressions near the downstream corner. The velocity measurements presented in Weber et al. (2001) also show that indeed some 3D effects in the velocity fields are present, even in the tributary. The flow fields presented for q=0.75 show some differences in magnitude and orientation of the near-bed and near-surface velocity vectors. Therefore, as already indicated in the discussion of the results, this effect should be considered when interpreting the pictures from the streamline visualization. The effect of the vertical differences in velocities on the results presented in this paper was checked in a selection of profiles, by measurement of transects at several heights. While indeed differences between the flow velocities at different depth were encountered, the velocities at 60% depth showed to be adequately representative of the depth-averaged flow.

7 CONCLUSION

The experiments performed confirmed the existence of significant upstream effects in the tributary induced by the confluence. The flow coming from the tributary has to make a 90° change in direction, and thus curvature of the streamlines becomes pronounced in the confluence zone. Associated with the streamline curvature, a local super-elevation near the upstream confluence corner forms. This super-elevation is clearly observable in the measurements. Because of the super-elevation, the flow is locally slowed down by the pressure gradient, which is also clearly visible in the velocity measurements, and therefore forms the flow stagnation zone. At the opposing wall, the streamlines contract, and the flow accelerates. Because the head losses are low, the total head is comparable to the upstream head in the uniform inlet section. Since the local velocities are increasing, the velocity height increases and thus the water depth decreases.

Comparison with the free vortex profile encountered near the transition of straight to curved channel in river bend flumes, showed that for high relative flow rates (like e.g. q=0.75), the theoretical free vortex velocity profile is a good approximation of the measured velocity profiles. The largest discrepancies exist near the left wall, where the flow decelerates more than the theoretical velocity profile predicts. For the lower flow rates (like e.g. q=0.25) the profile gave adequate predictions in the zone of flow acceleration, but underestimated the flow deceleration near the left wall.

Water depths in the tributary are found to be directly related to this velocity profile, because the low energy losses, the total head is conserved, and local water depths follow from the velocity head.

The overall flow and velocity redistribution thus clearly is initiated at a significant distance upstream of the confluence, and based on the findings in this paper upstream effects can be expected to exist up to a channel width upstream in the tributary.

Therefore, the influence of these upstream effects should be appropriately considered when discussing hydrodynamic processes in a confluence.

REFERENCES

Best, J. L. 1985. *Flow dynamics and sediment transport at river channel confluences*. Ph.D. thesis. London: University of London.

Biron, P., Best, J.L. and Roy, A.G., 1996. Effects of bed discordance on flow dynamics at open channel confluences. *Journal of Hydraulic Engineering*, 122(12), pp.676-682.

Creëlle, S., Schindfessel, L., & De Mulder, T. Modelling the tributary momentum contribution for predicting confluence head losses. Submitted to *Journal of Hydraulic Research.*

Đorđević, D. 2012 Application of 3D numerical models in confluence hydrodynamics modelling. in *XIX International Conference on Water Resources, 8p*.

Gurram, S. K. and Karki, K. S. 1997 Subcritical junction flow. *Journal of Hydraulic Engineering, 123*, pp. 447-455.

Hager, W. 1989 Transitional Flow in Channel Junctions. *Journal of Hydraulic Engineering, 115*(2), pp. 243-259.

Hsu, C.-C., Wu, F.-S. and Lee, W.-J. 1998 Flow at 90 equal-width open-channel junction. *Journal of Hydraulic Engineering, 124*(2), pp. 186-191.

Huang, J., Weber, L.J. and Lai, Y.G., 2002. Three-dimensional numerical study of flows in open-channel junctions. *Journal of hydraulic engineering*, 128(3), pp.268-280.

Modi, P. N., Dandekar, M. M. and Ariel, P. D. 1981 Conformal mapping for channel junction flow. *Journal of the Hydraulics Division, 107*(12), pp. 1713-1733.

Ramamurthy, A., Carballada, L. and Tran, D. 1988 Combining Open Channel Flow at Right Angled Junctions. *Journal of Hydraulic Engineering, 114*(12), pp. 1449-1460.

Rhoads, B. L. and Sukhodolov, A. N. 2008 Lateral momentum flux and the spatial evolution of flow within a confluence mixing interface. *Water Resources Research, 44*(8), pp. W08440, 17p.

Rozovskiĭ, I. L. v. 1957 *Flow of water in bends of open channels*, Academy of Sciences of the Ukrainian SSR.

Schindfessel, L., Creëlle, S. & De Mulder, T. 2015. Flow patterns in an open channel confluence with increasing-ly dominant tributary inflow. Water: 7(9): 4724-4751.

Taylor, E.H., 1944. Flow characteristics at rectangular open-channel junctions. *Transactions of the American Society of Civil Engineers*, 109(1), pp.893-902.

Webber, N. B. and Greated, C. 1966 An investigation of flow behaviour at the junction of rectangular channels. in *ICE Proceedings*: Thomas Telford. pp. 321-334.

Weber, L., Schumate, E. and Mawer, N. 2001 Experiments on Flow at a 90° Open-Channel Junction. *Journal of Hydraulic Engineering, 127*(5), pp. 340-350.